Stability of Zeolitic-imidazolate Frameworks in Humid Environments: Disentangling the Roles of Confined vs. Surface Water

Mohammad R. Momeni* and Farnaz A. Shakib*

Department of Chemistry and Environmental Science, New Jersey Institute of Technology, Newark 07102, NJ United States

Received September 12, 2020; E-mail: momeni@njit.edu,shakib@njit.edu

Abstract: Most of the chemistry in nanoporous materials with small pore sizes and windows are known to occur on the surface of the material which is in immediate contact with substrate/solvent, rather than inside the pores and channels. Experimentally, it is not straightforward to distinguish the chemistry of confinement from the surface. Comprehensive molecular dynamics simulations coupled with quantum mechanical calculations are employed to decipher stability of zeolitic-imidazolate frameworks in aqueous solutions. Water adsorption properties are compared and contrasted in crystalline bulk vs. nanopoarticles of ZIF-8 as a representative of the ZIF family in order to fully disentangle how water interacts with the surface of the material which contains coordinatively unsaturated metal sites compared to the pristine bulk. Our following detailed mechanistic study reveals the significantly higher propensity of the surface with coordinatively unsaturated Zn^{2+} sites toward water attack and hydrolysis. Our results presented in this work are general and are applicable to other nanoporous materials with small particle sizes, pores and windows and are useful in devising plans for synthesis of more robust water stable materials for applications that involve atmospheric and/or bulk water.

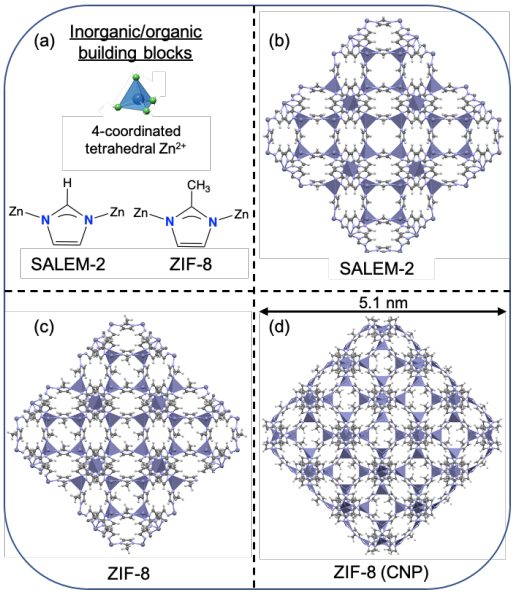

Figure 1. Molecular building blocks of SALEM-2 and ZIF-8 (a), 2×2×2 cubic crystal structures of SALEM-2 ($a = b = c = 33.661$ Å, 1632 atoms) (b) and ZIF-8 ($a = b = c = 33.982$ Å, 2208 atoms) (c) as well as a 5.1 nm crystalline nanoparticle (CNP) model of ZIF-8 with exposed edges and open-Zn^{2+} sites (3865 atoms) (d).

Introduction: Zeolitic-imidazolate frameworks (ZIFs),[1,2] one particularly interesting subclass of metal-organic frameworks (MOFs),[3,4] are chemically tunable permanently porous materials built by forming coordinative bonds between tetrahedral Zn^{2+} and/or Co^{2+} ions and imidazolate linkers which possess great potential applications in storage,,[5] chemical sensing,[6] separation,[7,8] encapsulation and controlled delivery,[9] as well as water harvesting[10,11] and catalysis[12,13] (Figure 1). It is now well established that majority of the catalysis occurs on the surface of the catalytic materials which are in immediate contact with substrates rather than inside pores/channels. That is the main reason why small particle sizes with uniform shapes are more desirable.[14] For example, ZIF-8 is experimentally shown to be hardly catalytically active in presence of bulky substrates which is attributed to the rather small pores and apertures of this material.[15] Despite all these intriguing findings, most studies on ZIF-8 and other porous materials in general have focused on bulk crystalline models and ignored the effects of particle sizes/shapes and external surface areas. In a recent seminal work of Pang et al.[14] on hydrolytic stability of ZIF-8 nanoparticles under different neutral/acidic conditions it was found that under mild acidic conditions of wet SO_2, hydrolysis manily occurs on the surface of the particles with their core staying intact. X-ray photoelectron, FTIR and XPS spectra as well as the SEM and TEM images of the as-prepared and acid-gas degraded samples confirmed the hydrolysis and formation of $Zn(OH)_2$ like species and protonated imidazolate linkers on the surface of the nanoparticles.[14] While several experimental studies have highlighted the promising potential of ZIFs in aqueous solutions or in the presence of atmospheric water, a full atomistic level understanding of the underlying interatomic interactions between water and these framework and their possible dissolution in aqueous solutions is still missing.

Here, a combined quantum mechanics/molecular dynamics approach is employed to fully investigate the structure, dynamical and thermodynamical properties of water in confined nanopores as well as on the surfaces of ZIF-8 as a representative of the ZIF family. To this end, both crystalline bulk (CB) and crystalline nanoparticle (CNP) models with grain boundaries and exposed surfaces/edges and under-coordinated Zn^{2+} metal centers are considered. Our simulations are aimed to investigate (i) how water interacts with the framework, (ii) how it nucleates and grows droplets inside confined spaces of the nanopores vs. the surface/edge of these materials, and (iii) whether its properties resemble properties of bulk water in condensed or gas phases. We compared our results for bulk ZIF-8 to that of SALEM-2 with similar sodalite topology to test the transferability of our developed force field and, more importantly, check the effect of steric hinderance around the Zn^{2+} metal centers on

the propensity of the framework to hydrolysis (see Supporting Information (SI) for details of our methodology). Our comprehensive MD simulations with different water loadings reveal adsorption of water molecules by the frameworks of SALEM-2 and ZIF-8 occur via forming a penta-coordinated complex with the Zn^{2+} metal centers which becomes more favorable as water loading increases. Detailed mechanistic study using accurate periodic and cluster electronic structure calculations shows that water induced Zn^{2+}-imidazolate hydrolysis is more favored on the surface of the material which contains coordinatively unsatureated metal sites than in bulk. Our findings in this work are general and applicable to other ZIFs and nanoporous materials and are of increasing relevance to materials with small particle sizes, pores and apertures where surface-to-volume ratio is high.

Results and Discussion: It is now well established that a material's particle size/shape and the presence and density of the open-metal sites is a crucial factor in applications such as adsorption, separation and catalysis. That is the sole reason why achieving lower particle sizes with uniform shapes is always desirable. It is therefore clearly important to take into account the presence of surfaces/edges with under-coordinated metal sites especially when the pores and apertures of the studied material are too small to allow the substrates and other guest molecules to freely enter the pores. In this work, we address this gap in the literature via building a realistic 5.1 nm crystalline nanoparticle (CNP) of ZIF-8, based on experimentally available data such as SEM/TEM images and measured surface areas, and compared its properties to an extended crystalline bulk (CB) model with no defects, surfaces or edges.

Structural characterization of confined vs. surface water: In our previous studies we have highlighted the importance of the presence of missing linker defects with open-metal sites on catalytic activity of different MOFs.[16–20] Our detailed mechanistic studies showed that the first catalytic step is always activation of the substrates by their coordination to these open-metal sites. Most theoretical studies use periodic boundary conditions on perfect pristine crystalline bulk models and neglect the presence of these surfaces/edges that are in immediate contact with substrates and solvents. As mentioned above, we have considered two different models in this work, in one model we built pristine 2×2×2 models of SALEM-2 and ZIF-8 from their corresponding available experimental data while for the other model we built a ≈ 5.1 nm CNP of ZIF-8 by building a 4×4×6 supercell of ZIF-8 and cutting the outermost imidazolate linkers (Figures 1 and 2. The latter is therefore consist of exposed edges/surfaces and under coordinated Zn^{2+} metal centers. Classical MD simulations using our newly developed force field were then performed at 300 K and 1 atm pressure with using the periodic boundary conditions on these models the results of which for both dry and hydrated systems are illustrated in Figure 2 (see SI section S1 for more details).

1-4 H_2O molecules per Zn^{2+} metal centers were equilibrated in the cases of the CB ZIF-8 and SALEM-2 systems (corresponding to 96, 192, 288 and 384 water molecules, respectively) whereas for the ≈ 5.1 nm CNP of ZIF-8 we equilibrated 1-3 H_2O molecules per Zn^{2+} atoms (corresponding to respectively, 192, 384 and 576 water molecules). For the latter, water molecules were equilibrated both inside (hereafter referred as "confined water", Figure 2c) and outside (hereafter referred as "surface water", Figure 2d). The calculated Zn-O_W and H_W-N radial distribution functions (RDFs) for

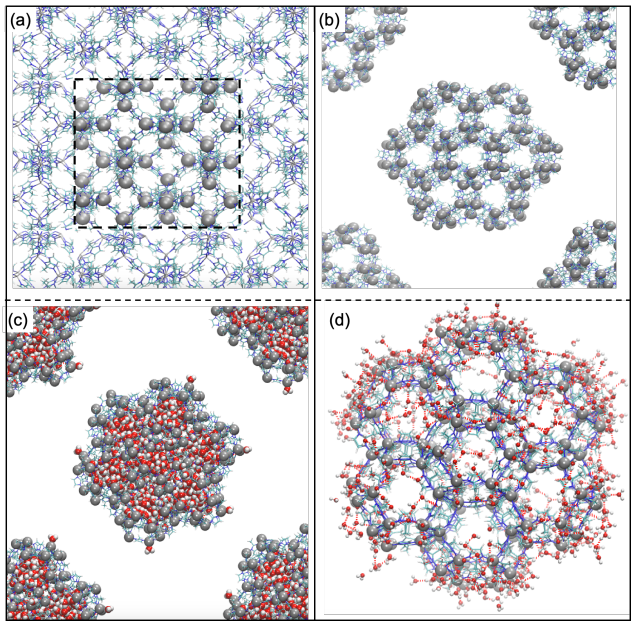

Figure 2. Periodic images of the MD snapshots of the dry 300 K MD equilibrated (a) CB and (b) CNP models of ZIF-8; MD snapshots of the hydrated nanocrystal model of ZIF-8 with 576 water molecules equilibrated inside (confined water) (c) and outside (surface water) (d). In (a) the unit cell is highlighted with black dashed lines.

different hydrated CB models of ZIF-8 and SALEM-2 are given in Figure 3. Calculated Zn-N RDFs in both ZIF-8 and SALEM-2 are within ±0.02 Å of both experimentally determined and our *ab initio* PBE-D3 optimized bond distances (see SI Figure S1 for the experimental and PBE-D3 optimized structures of SALEM-2 and ZIF-8 and Figure S4 for the Zn-N RDFs). Also, the size of the 5 ns MD equilibrated unit cell vectors for the studied cubic unit cells of both bulk SALEM-2 and ZIF-8 are in excellent agreement with their corresponding experimentally measured and our *ab initio* PBE-D3 optimized values (i.e. +0.7% for dry SALEM-2 and +0.6% for dry ZIF-8 compared to their experimentally measured values) (SI Figure S4).

Interestingly, in both CB and CNP models of ZIF-8 and CB model of SALEM-2, calculated RDF peaks for Zn-O_W bond show a prominent peak at ≈ 2.3 Å corresponding to the formation of a pentacoordinated complex (Figures 3(a), 3(c) and 3(e)). In the case of the CNP, all undercoordinated Zn^{2+} metal centers are coordinated to two water molecules with their Zn-O_W RDF peaks down-shifted by ≈ 0.1 Å. Inspecting the H_W–N RDF peaks show a peak at ≈3 Å corresponding to H-bond formation between water molecules and nitrogen atoms of the imidazolate linkers. We will further discuss the importance of the formation of these Zn-O_W and H_W–N bonds in the next section where we discuss hydrolysis of Zn^{2+}-Im bonds in ZIFs.

Figures 3(g)–3(j) show the percentage of water molecules coordinated to the Zn^{2+} centers (Zn_{coord}), hydrogen bonded to one (Im_{HB}) and two (Im_{HB-2}) imidazolate linkers as well as the percentage of free (W_F) water molecules. As can be seen from Figure 3(g) and 3(h), the percentage of Zn_{coord} in bulk ZIF-8 is less than 1/3 of that of bulk SALEM-2 (i.e. 28.4% vs 8.6%) for 96 water molecules. The lower percentage of the Zn_{coord} species in bulk ZIF-8 is likely due to the presence of the bulky methyl groups which can protect the metal sites from water attacks by providing steric hindrance.

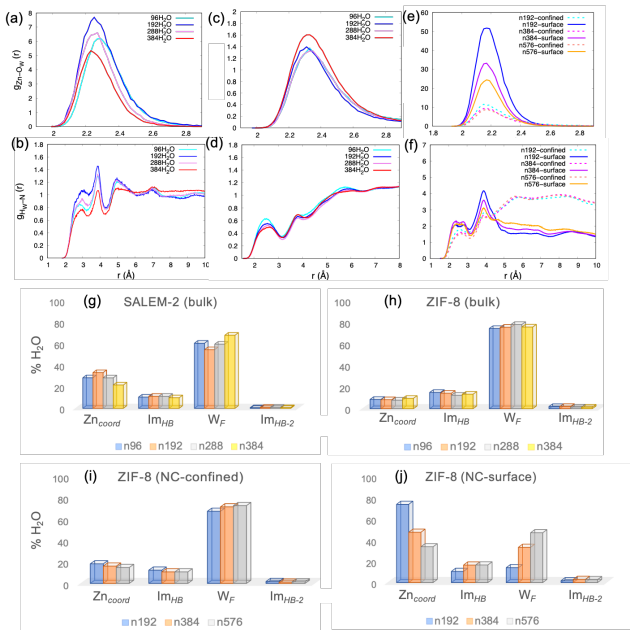

Figure 3. Calculated RDFs for Zn-O_W and H_W-N bonds in CB SALEM-2 ((a) and (b)) as well as CB ((c) and (d)) and CNP ((e) and (f)) models of ZF-8 with different water loadings. Calculated percentage of water molecules coordinated to one Zn^{2+} center (Zn_{coord}), hydrogen bonded to one (Im_{HB}) and two (Im_{HB-2}) imidazolate linkers as well as free water molecules (W_F) in CB SALEM-2 (g) CB ZIF-8 (h) and CNP ZIF-8 ((i) and (j)) over an entire 1 ns MD trajectory in the NPT ensemble. For changes in absolute number of water molecules see SI Figures S1 and S2.

However, as more water molecules are added to the simulation box this ratio drops to 21.7% vs 9.6% for 384 water molecules which show water coordination becomes thermodynamically more favored at higher water concentrations. In the case of bulk ZIF-8 the percentage of Im_{HB} species is almost twice that of the Zn_{coord} while opposite is true in the case of bulk SALEM-2. Considering CNP, there can be seen a significant difference between these isomers when the same water/metal ratio is equilibrated inside (confined water) or outside (surface water) the CNP. The calculated percentages of the surface water greatly depend on the concentration of water molecules. For example, going from 192 H_2O to 576 H_2O the percentage of Zn_{coord} drops by more than a factor of two, i.e. from 73.7% to 33.7%. Analysis of our MD trajectories show that some of the penta-coordinated complexes on the surface are formed with two water molecules coordinated to the same metal center. These water molecules then break free and increase W_F from 14% to 46.9%. It is noteworthy that some of these released water molecules form H-bond complexes with the imidazolate linkers as evident from the rise of Im_{HB} from 10.5% to 16.6% going from 192 H_2O to 576 H_2O molecules (Figure 3(j)). The percentage increase/decrease in the different types of water molecules in NC-confined ZIF-8 system is small and follows the trend observed for bulk ZIF-8; nevertheless, the percentage of Zn_{coord} is about 6% larger than the Im_{HB} species (Figure 3(i)).

Thermodynamical and dynamical properties of surface vs. confined water: To gain further insight on the behavior of confined vs. surface water, we calculated different dynamical as well as thermodynamical properties of water. The calculated water reorientation relaxation time (τ_2) and total self diffusivity (D_{tot}) as well as heat of adsorption (E_{ads}) of different ZIFs are tabulated in Table 1. We calculated the dynamical properties (τ_2 in ps and D_{tot} in ps/Å^2) over an ensemble of 10 independent NVE trajectories, each with a duration of 50 ps starting from randomly generated configurations from 10 ps canonical ensemble NVT simulations. We calculated D_{tot} based on mean square displacement of the particles[25] using the following equation:

$$D = \lim_{t\to\infty} \frac{1}{6t}\langle(\mathbf{r}(t) - \mathbf{r}(0))^2\rangle \quad (1)$$

Diffusion coefficients along different x, y and z directions were also calculated for different water loadings but no significant difference was observed and hence only the total diffusion coefficient values are reported for all studied systems. We quantified water reorientation relaxation in terms of the orientational time correlation functions (TCFs). We formulated TCFs in terms of the reorientation of the unit vector $\hat{\mathbf{u}}_{OH}$ that lies along one of the OH bonds of a water molecule:

$$C_{2,\mathrm{OH}}(t) = \langle P_2[\hat{\mathbf{u}}_{\mathrm{OH}}(0)\hat{\mathbf{u}}_{\mathrm{OH}}(t)]\rangle \quad (2)$$

where P_2 is the Legendre polynomial of order 2. The time dependence of the 2^{nd} Legendre polynomial is exponential and can be used to determine orientational relaxation time (τ_2):

$$C_{2,\mathrm{OH}}(t) \propto \exp(-\frac{t}{\tau_2}). \quad (3)$$

The heat of adsorption (E_{ad}) for different ZIFs were calculated per water molecule using the following equation:

$$E_{ad} = \frac{1}{n}\{E_{n@ZIF} - [E_{ZIF} + E_n]\} \quad (4)$$

where E_{ZIF} and $E_{n@ZIF}$ refer to the total energy of different dry and hydrated ZIFs with n being the number of water molecules. The total energy of the isolated water molecules (E_n) was calculated by equilibrating n water molecules in the same simulation box but in the absence of the ZIF framework. All calculated dynamical and thermodynamical properties for different water loadings point to greater water interactions with bulk SALEM-2 framework than that of bulk ZIF-8. For example, calculated τ_2 values for bulk SALEM-2 plateau at 47.1 ps for 4 H_2O per Zn^{2+} while the corresponding value for bulk ZIF-8 is 36.2 ps. Considering the experimentally measured τ_2 values for bulk water (1.7–2.6 ps[21–23]), these data clearly signal that water is more free in CB ZIF-8 than CB SALEM-2 though significantly limited compared to the bulk water. The computed τ_2 values combined with the total diffusion coefficients clearly illustrate rather strong interaction of water molecules with the frameworks as outlined in the previous section. Similar trend can be observed for the calculated total diffusion coefficients (Table 1). In agreement with the dynamical properties, calculated ther-

Table 1. Computed water reorientation relaxation time (τ_2 in ps), total self diffusivity (D_{tot} in ps/Å^2) and heat of adsorption (E_{ads} in kcal/mol) for CB SALEM-2 and ZIF-8 as well as CNP model of ZIF-8 with different water loadings at 300 K. Experimentally measured values for bulk water are given for comparison.

ZIF Systems	SALEM-2 (CB)			ZIF-8 (CB)		
Water Molecules	τ_2	D_{tot}	E_{ads}	τ_2	D_{tot}	E_{ads}
1 H_2O/Zn^{2+}	52.4	0.012	−3.8	29.7	0.044	−1.0
2 H_2O/Zn^{2+}	63.7	0.011	−4.7	27.6	0.045	−1.1
3 H_2O/Zn^{2+}	47.8	0.013	−4.7	23.4	0.043	−1.4
4 H_2O/Zn^{2+}	47.1	0.018	−4.0	36.2	0.028	−1.8
	ZIF-8 (CNP–confined)			**ZIF-8 CNP–surface)**		
Water Molecules	τ_2	D_{tot}	E_{ads}	τ_2	D_{tot}	E_{ads}
1 H_2O/Zn^{2+}	25.3	0.062	−2.7	45.2	0.046	−8.6
2 H_2O/Zn^{2+}	25.2	0.046	−2.4	47.1	0.094	−5.8
3 H_2O/Zn^{2+}	24.3	0.088	−3.5	36.3	0.133	−5.2
Exp. bulk water	1.7–2.6[21–23]	0.229[24]				

modynamical heat of adsorption (E_{ad}) for bulk SALEM-2 are by more than a factor of two larger than the corresponding values for bulk ZIF-8 over all studied water loadings (Table 1). As more water molecules are added to the simulation box by going from 1 H_2O / Zn^{2+} to 4 H_2O / Zn^{2+} one can see a rise in the calculated E_{ad} for both bulk ZIF-8 (from –1.0 kcal/mol to –1.8 kcal/mol) and bulk SALEM-2 (from –3.8 kcal/mol to –4.0 kcal/mol, Table 1). Once coordinated water donates one or both of its hydrogen atoms to the nearby water molecules it can form a stronger coordinative bond with the metal center. This cooperative effects of water lead to the increasing trend of E_{ad} with respect to water loading and will be further discussed when outlining the results of our quantum mechanical calculations. Analysis of the computed E_{ad} for surface water in CNP shows a decreasing trend from –8.6 to –5.2 going from 1 H_2O to 3 H_2O molecules per Zn^{2+} centers. Combined with the decrease and increase in the computed τ_2 and D_{tot}, respectively, it shows that as more water is added to the outer sphere of the CNP more bulk-like behavior is observed from water (Figure 3 and Table 1). As water saturates the under-coordinated Zn^{2+} centers present on the surface of the CNP, the extra water molecules can only form H-bonds with Zn_{coord} in the first and higher solvation shells (Figure 4). The M06-L optimized tetra- and three-coordinated cluster models of ZIF-8 cut from the MD equilibrated dry system are shown in Figure 4.

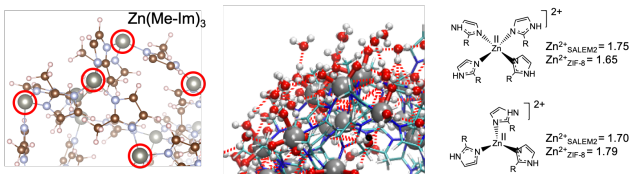

Figure 4. Surfaces/edges of the equilibrated dry (left) and hydrated (center) CNP with under-coordinated Zn^{2+} metal centers highlighted with red circles on the left. The M06-L optimized tetra- and three-coordinated cluster models cut from the equilibrated dry system with the M06-2X(SMD, water) computed CHELPG charges on the Zn^{2+} metal centers are given on the right.

The M06-2X(SMD, water) computed CHELPG charges on the Zn^{2+} metal centers show a higher positive charge on the Zn^{2+} center of SALEM-2 compared to ZIF-8 in the tetra-coordinated complexes (+1.75 e vs +1.65 e) while in the three-coordinated complexes the order is reversed (+1.70 e vs +1.79 e). This clearly shows that surface of ZIF-8 is more susceptible to water attack and hydrolysis than the surface of SALEM-2. This also agrees with the higher E_{ad} values computed from our MD simulations in the CNP than its BC model (Table 1). Overall, one can conclude that when water molecules are packed inside the NC model they behave more or less similar to bulk ZIF-8 but once they are placed on the surface of the material the behavior of water changes completely. For example, W_F in the highest water loading is down to 46.9% compared to 78% in the CB ZIF-8. Also, as more water is added to the simulation box two opposite effects are observed for confined vs. surface water: surface water molecules take of bulk water characteristics while confined water molecules show cooperative effects and interact stronger with the framework as can be seen from the increase in the computed E_{ad} values.

Reactivity of surface vs. bulk water in hydrolysis of ZIF-8: As mentioned before, the occurrence of missing linker defects with open-metal sites is crucial for most bond forming and breaking reactions catalyzed by porous materials. Based on available experimental data and structural, thermodynamical and dynamical properties obtained from our extensive MD simulations, we propose a three step mechanism for hydrolysis of ZIFs as following: (i) water addition to the Zn^{2+} metal centers (water addition step); (ii) imidazolate linker displacement by the coordinated water molecule (water displacement step); and (iii) proton transfer from the coordinated water to the H-bonded imidazolate linker to form the final Zn-OH complex (Figure 5(a)). This mechanism is consistent with the FTIR spectroscopic data from Pang et al.[14] where they found hydrolysis leads to the formation of Zn-OH like species on the surface of the ZIF-8 nanoparticles. The M06-2X/def2-TZVP computed mechanistic scheme is given in Figure 5(b).

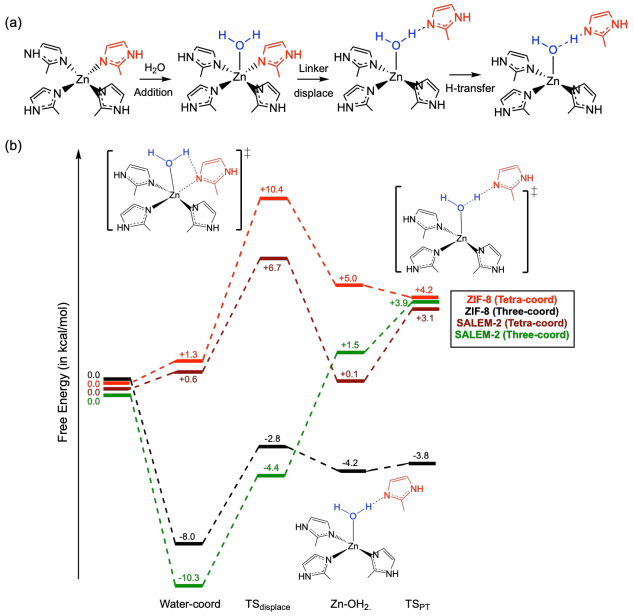

Figure 5. (a) Proposed mechanistic scheme for hydrolysis of ZIF-8 and (b) M06-2X(SMD)/def2-TZVP//M06-L/def2-SVP(gas) 298 K calculated free energies for hydrolysis of both the three- and tetra-coordinated complexes of ZIF-8 and SALEM-2. Separated reactants form the zero of energy. Key reactant and transition states for ZIF-8 are shown.

For this mechanism, both the four- and three-coordinated complexes as depicted in Figure 4 were considered. Comparison between the reactivity of these two complexes tells us about the susceptibility of core vs surface of the material toward water attack and hydrolysis. Comparison between the M06-2X(SMD, Water) computed free energy changes (ΔGs) for the first step of the mechanism outlined in Figure 5 (i.e. addition of water to the Zn^{2+} centers) to the computed E_{ad} values from our MD simulations confirms the existence of a remarkable agreement between our quantum mechanical calculations and classical MD simulations. For example, our computed E_{ad} values for CNP surface (–8.6 kcal/mol, Table 1) is in close agreement with our M06-2X(SMD, Water)/def2-TZVP computed values for the unsaturated three-coordinated complexes of ZIF-8 (–8.3 kcal/mol, Figure 5(b)). In both tetra- and three-coordinated complexes, our M06-2X(SMD, water) computed ΔGs for addition of water to the Zn^{2+} centers is higher for SALEM-2 than ZIF-8 in qualitative agreement with the computed E_{ad} values from our MD simulations (see Figure 5(b) and Table 1). Quantum mechanical calculations show that in the case of the mono-hydrated tetra-coordinated complex of ZIF-8

water only weakly interacts with the imidazolate linkers and does not bind to the Zn^{2+} center. After two additional water molecules are H-bonded to the initial water molecule, it forms a coordinative bond with the Zn^{2+} center (see Figure 6).

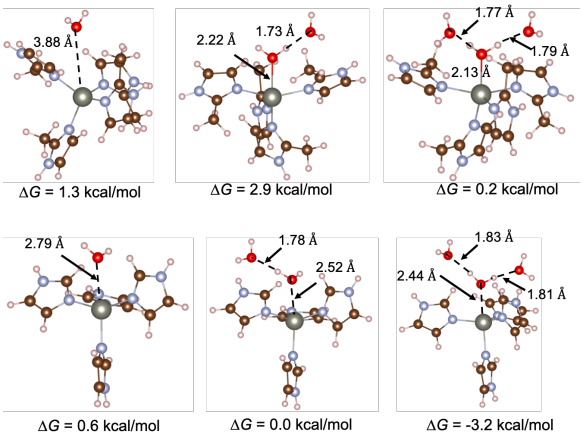

Figure 6. Key bond lengths (Å, M06-L) in cluster-model structures for water addition to ZIF-8 (top) and SALEM-2 (bottom). M06-2X(SMD, Water) calculated changes in free energies upon addition of water are given; isolated species are considered as zero of energy.

For SALEM-2 the change is more significant upon addition of extra water molecules; from 0.6 kcal/mol to –3.2 kcal/mol (Figure 6). It is worthwhile mentioning that these values form an upper bound to the change in free energies for addition of water but nevertheless confirm the cooperative effect observed in the computed E_{ad} values in the previous section. The second step (i.e. the displacement of the imidazolate linkers by the coordinated water molecule) was found to be the rate-determining step in both ZIF-8 and SALEM-2 with computed free energy barriers ($\Delta G^{\ddagger}$s) of +10.4 kcal/mol and 6.7 kcal/mol, respectively for the tetra-coordinated complexes. This is in agreement with our previous studies on heterogeneous catalytic hydrolysis of nerve agents using different Zr^{IV}–MOFs where it was found that among the considered steps coordination and displacement of water by the nerve agent is the rate-determining step of the reaction.[16–18] Interestingly, in the three-coordinated complex of SALEM-2, the computed $\Delta G^{\ddagger}$ stays almost the same (i.e. +6.0 kcal/mol) while the computed $\Delta G^{\ddagger}$ for the analogues complex of ZIF-8 is cut to half (+5.2 kcal/mol) which is even lower than that of SALEM-2 by 0.8 kcal/mol. That is remarkable given the fact that as mentioned above Pang et al. have shown that hydrolysis only occurs on the surface of ZIF-8 with the core of the nanoparticles staying intact.[14] The calculated changes in $\Delta G^{\ddagger}$ correlate well with the computed RESP charges on the Zn^{2+} metal centers of the dry three- and tetra-coordinated complexes of SALEM-2 and ZIF-8 (Figure 4). Based on these results, we anticipate that use of surface masking agents and/or functionalizing the imidazolate linkers with more bulky substituents are possible ways of achieving higher water stabilities for ZIFs and other related materials. Future works will be focused on finding useful structure and/or energy descriptors such as Zn–OH_2 bond orders and electrophilicities, which are much more readily computed than the full reaction path, for future screening of water stable ZIFs for desired applications.

Conclusions: Lack of an atomostic level understanding of the mechanisms by which nanoporous ZIFs interact with the surrounding environments is hindering development of more effective materials for desired applications in aqueous solutions. Here, through extensive analysis of structural properties and hydrogen bonding motifs, our combined quantum mechanical / classical MD simulations examine water adsorption in both nanoconfinement as well as on the surface of ZIF-8. It was found that water prefers to bond to the Zn^{2+} metals in both ZIF-8 and SALEM-2 by forming a penta-coordinated complex which can then lead to the dissociation of the Zn-Imidazolate bond and overall hydrolysis of these materials. We also found that surface of ZIF-8 with under-coordinated Zn^{2+} centers is significantly more susceptible to hydrolysis than bulk which agrees very well with available experimental data. Findings from this study will inspire fundamental design principles for more robust functional materials with superior water stabilities in aqueous solutions.

Computational methods: Details of the computational methodology used in this article are provided in the SI Appendix. These methods include developing *ab initio* force fields, validation of the force fields, details of the classical molecular dynamics simulations, and details of the periodic and cluster quantum mechanical calculations. The DL_POLY_2,[26] CP2K version 5.1.,[27] Gaussian 16 Revision A.03,[28] and QCHEM 5.2.[29] software packages were used for these calculations.

Supporting Information Available

Details of our flexible *ab initio* force fields, results of our classical MD simulations and quantum mechanical calculations as well as XYZ coordinates of all systems.

Acknowledgement FAS is grateful for receiving a startup budget from NJIT. This work used the Extreme Science and Engineering Discovery Environment (XSEDE), which is supported by National Science Foundation grant number CHE200007 and CHE200008. This research has been (partially) enabled by the use of computing resources provided by Kong HPC center at NJIT. MRM thanks Sara Abdelhamid for her help during this project.

References

(1) Huang, X.-C.; Lin, Y.-Y.; Zhang, J.-P.; Chen, X.-M. Ligand-Directed Strategy for Zeolite-Type Metal–Organic Frameworks: Zinc(II) Imidazolates with Unusual Zeolitic Topologies. *Angew. Chem. Int. Ed.* **2006**, *45*, 1557–1559.

(2) Park, K. S.; Ni, Z.; Côté, A. P.; Choi, J. Y.; Huang, R.; Uribe-Romo, F. J.; Chae, H. K.; O'Keeffe, M.; Yaghi, O. M. Exceptional chemical and thermal stability of zeolitic imidazolate frameworks. *PNAS* **2006**, *103*, 10186–10191.

(3) Furukawa, H.; Cordova, K. E.; OKeeffe, M.; Yaghi, O. M. The Chemistry and Applications of Metal-Organic Frameworks. *Science* **2013**, *341*, 1230444.

(4) Yaghi O. M.; O′Keeffe, M.; Ockwig, N. W.; Chae, H. K.; Eddaoudi, M.; Kim, J. *Nature*, **2003**, *423*, 705-714.

(5) Banerjee, R.; Phan, A.; Wang, B.; Knobler, C.; Furukawa, H.; O'Keeffe, M.; Yaghi, O. M. High-Throughput Synthesis of Zeolitic Imidazolate Frameworks and Application to CO2 Capture. *Science* **2008**, *319*, 939–943.

(6) Lu, G.; Hupp, J. T. MetalOrganic Frameworks as Sensors: A ZIF-8 Based FabryPérot Device as a Selective Sensor for Chemical Vapors and Gases. *J. Ame. Chem. Soc.* **2010**, *132*, 7832–7833.

(7) Li, K.; Olson, D. H.; Seidel, J.; Emge, T. J.; Gong, H.; Zeng, H.; Li, J. Zeolitic Imidazolate Frameworks for Kinetic Separation of Propane and Propene. *J. Am. Chem. Soc.* **2009**, *131*, 10368–10369.

(8) Chang, N.; Gu, Z.-Y.; Yan, X.-P. Zeolitic Imidazolate Framework-8 Nanocrystal Coated Capillary for Molecular Siev-

ing of Branched Alkanes from Linear Alkanes along with High-Resolution Chromatographic Separation of Linear Alkanes. *J. Am. Chem. Soc.* **2010**, *132*, 13645–13647.
(9) Liédana, N.; Galve, A.; Rubio, C.; Téllez, C.; Coronas, J. CAF@ZIF-8: One-Step Encapsulation of Caffeine in MOF. *ACS Appl. Mater. & Interfaces* **2012**, *4*, 5016–5021.
(10) Kim, H.; Yang, S.; Rao, S. R.; Narayanan, S.; Kapustin, E. A.; Furukawa, H.; Umans, A. S.; Yaghi, O. M.; Wang, E. N. Water harvesting from air with metal-organic frameworks powered by natural sunlight. *Science* **2017**, *356*, 430–434.
(11) Hanikel, N.; Prévot, M. S.; Fathieh, F.; Kapustin, E. A.; Lyu, H.; Wang, H.; Diercks, N. J.; Glover, T. G.; Yaghi, O. M. Rapid Cycling and Exceptional Yield in a Metal-Organic Framework Water Harvester. *ACS Cent. Sci.* **2019**, *5*, 1699–1706.
(12) Chen, B.; Yang, Z.; Zhu, Y.; Xia, Y. Zeolitic imidazolate framework materials: recent progress in synthesis and applications. *J. Mater. Chem. A* **2014**, *2*, 16811–16831.
(13) Cheng, N.; Ren, L.; Xu, X.; Du, Y.; Dou, S. X. Recent Development of Zeolitic Imidazolate Frameworks (ZIFs) Derived Porous Carbon Based Materials as Electrocatalysts. *Adv. Energy Mater.* **2018**, *8*, 1801257.
(14) Pang, S. H.; Han, C.; Sholl, D. S.; Jones, C. W.; Lively, R. P. Facet-Specific Stability of ZIF-8 in the Presence of Acid Gases Dissolved in Aqueous Solutions. *Chem. Mater.* **2016**, *28*, 6960–6967.
(15) Chizallet, C.; Lazare, S.; Bazer-Bachi, D.; Bonnier, F.; Lecocq, V.; Soyer, E.; Quoineaud, A.-A.; Bats, N. Catalysis of Transesterification by a Nonfunctionalized MetalOrganic Framework: Acido-Basicity at the External Surface of ZIF-8 Probed by FTIR and ab Initio Calculations. *J. Am. Chem. Soc.* **2010**, *132*, 12365–12377.
(16) Momeni, M. R.; Cramer, C. J. Dual Role of Water in Heterogeneous Catalytic Hydrolysis of Sarin by Zirconium-Based Metal–Organic Frameworks. *ACS App. Mater. & Interfaces* **2018**, *10*, 18435–18439.
(17) Momeni, M. R.; Cramer, C. J. Structural Characterization of Pristine and Defective [Zr12(3-O)8(3-OH)8(2-OH)6]18+ Double-Node Metal–Organic Framework and Predicted Applications for Single-Site Catalytic Hydrolysis of Sarin. *Chem. Mater.* **2018**, *30*, 4432–4439.
(18) Momeni, M. R.; Cramer, C. J. Computational Screening of Roles of Defects and Metal Substitution on Reactivity of Different Single- vs Double-Node Metal–Organic Frameworks for Sarin Decomposition. *J. Phys. Chem. C* **2019**, *123*, 15157–15165.
(19) Yang, D.; Momeni, M. R.; Demir, H.; Pahls, D. R.; Rimoldi, M.; Wang, T. C.; Farha, O. K.; Hupp, J. T.; Cramer, C. J.; Gates, B. C.; Gagliardi, L. Tuning the properties of metal–organic framework nodes as supports of single-site iridium catalysts: node modification by atomic layer deposition of aluminium. *Faraday Discuss.* **2017**, *201*, 195–206.
(20) Kalaj, M.; Momeni, M. R.; Bentz, K. C.; Barcus, K. S.; Palomba, J. M.; Paesani, F.; Cohen, S. M. Halogen bonding in UiO-66 frameworks promotes superior chemical warfare agent simulant degradation. *Chem. Commun.* **2019**, *55*, 3481–3484.
(21) Winkler, K.; Lindner, J.; Bürsing, H.; Vöhringer, P. Ultrafast Raman-induced Kerr-effect of water: Single molecule versus collective motions. *J. Chem. Phys.* **2000**, *113*, 4674.
(22) Lawrence, C. P.; Skinner, J. L. Vibrational spectroscopy of HOD in liquid D2O. D 2 O . III. Spectral diffusion, and hydrogen-bonding and rotational dynamics. *J. Chem. Phys.* **2003**, *118*, 264.
(23) Rezus, Y. L. A.; Bakker, H. J. On the orientational relaxation of HDO in liquid water. *J. Chem. Phys.* **2005**, *123*, 114502.
(24) Krynicki, K.; Green, C. D.; Sawyer, D. W. Pressure and temperaturedependence of self-diffusion in water. *Faraday Discuss* **1978**, *66*, 199.
(25) Nitzan, A. *Chemical Dynamics in Condensed Phases: Relaxation, Transfer, and Reactions in Condensed Molecular Systems*; Oxford University Press, 2006.
(26) Smith, W.; Forester, T. DL_POLY_2.0: A general-purpose parallel molecular dynamics simulation package. *J. Mol. Graph.* **1996**, *14*, 136 – 141.
(27) Hutter, J.; Iannuzzi, M.; Schiffmann, F.; VandeVondele, J. cp2k: atomistic simulations of condensed matter systems. *WIREs Computational Molecular Science* **2014**, *4*, 15–25.
(28) Frisch, M. J., et al. Gaussian 16 Revision A.03. Gaussian Inc. Wallingford CT 2016.
(29) Shao, Y.; Gan, Z.; Epifanovsky, E.; Gilbert, A. T.; Wormit, M.; Kussmann, J.; Lange, A. W.; Behn, A.; Deng, J.; Feng, X., et al. Advances in molecular quantum chemistry contained in the Q-Chem 4 program package. *Mol. Phys.* **2015**, *113*, 184–215.

Graphical TOC Entry